JOURNAL OF MATERIALS SCIENCE 32 (1997) 6129–6133

Lead zirconate titanate thin films on GaAs substrates

S. ARSCOTT, R. KURCHANIA*, R. E. MILES, S. J. MILNE*
Microwave and Terahertz Technology Group, Department of Electronic and Electrical Engineering, The University of Leeds, Leeds LS2 9JT, UK
** School of Materials, The University of Leeds, Leeds LS2 9JT*

Thin films of the piezoceramic lead zirconate titanate (PZT) of composition $Pb(Zr_{0.53}Ti_{0.47})O_3$ have been prepared on a platinized GaAs substrate system using a propanediol based sol–gel technique. A Si_3N_4 buffer layer was deposited onto the GaAs by plasma-enhanced chemical vapour deposition so as to minimize Ga and As diffusion during film fabrication. Rapid thermal processing (RTP) techniques were used to thermally decompose the sol–gel layer to PZT in a further effort to avoid problems of Ga and As diffusion. Adhesion between the electrode and substrate was found to improve when an intermediate Ti layer deposited between the Pt and Si_3N_4 was oxidized prior to depositing the Pt layer. A crystalline PZT film was produced on the $Pt/TiO_2/Si_3N_4/GaAs$ by firing the sol–gel coating at 350 °C for 1 min and then at 650 °C for 10 s using RTP. A single deposition of precursor sol resulted in a film 0.5 μm thick. Measured average values of remanant polarization and coercive field were 14 $\mu C\,cm^{-2}$ and 47 $kV\,cm^{-1}$, respectively. The polarization value is rather low, as conventionally fired films on silicon have remanent polarization values of 20–30 $\mu C\,cm^{-2}$; the lower values may be due to incomplete crystallization during RTP, but a degradation of properties due to Ga–As diffusion, despite the precautions, cannot be ruled out at this stage.

1. Introduction

The electromechanical properties of the ferroelectric lead zirconate titanate $Pb(Zr_{0.53}Ti_{0.47})O_3$ PZT (53/47) [1] render it a candidate material for the fabrication of analogue microwave components such as bulk acoustic wave (BAW) resonators [2, 3] which can be integrated directly onto monolithic microwave integrated circuits (MMICs). To date, thin film technology for the fabrication of BAW devices has concentrated mainly on sputtered thin films of ZnO and AlN [4]; however, these possess rather low piezoelectric factors which restrict the bandwidth of filters that can be fabricated and increases the insertion loss. The use of ferroelectric thin films such as lead zirconate titanate (PZT) would offer greatly increased coupling factors, resulting in higher Q values for devices such as resonators and filters.

There are a number of thin-film deposition techniques available, but in recent years the sol–gel deposition method [5] has been widely used for manufacturing ferroelectric thin films since it can potentially achieve better control of composition in these multicomponent systems [6] than is possible using physical or chemical vapour deposition methods [7]. The sol–gel process utilizes a polymeric precursor sol prepared from metal acetates and alkoxides in an organic solvent; after coating onto a substrate the sol transforms to a gel layer which can be converted to a ceramic film by thermolysis in the temperature range 500–700 °C. Recent developments have shown that PZT films in the thickness range 0.5–1 μm can now be obtained via a single coating technique using a propanediol-based sol–gel system developed in this laboratory. This presents a significant advantage over a number of existing sol–gel routes [5] which require repeated coating–annealing steps to achieve thin films of a similar thickness. A PZT film thickness of 1 μm should permit a BAW device to be fabricated having an operational frequency in the region of 3 GHz, making the proapanediol sol–gel route an attractive method for depositing piezoceramic films for such applications.

For other PZT film applications such as ferroelectric memories, pyroelectric detectors and piezoelectric actuators, $Pt/Ti/SiO_2/Si$ is the most widely used substrate. The intermediate titanium layer acts as an adhesion layer between the platinum and a thermally grown silica layer.

For devices operating at microwave frequencies, the higher electron drift velocity, electron mobility and semi-insulating qualities of GaAs, relative to those values obtained for Si, make it the preferred choice for MMIC substrate material. However, because of the facile diffusion of As and Ga at the temperatures involved in sol–gel processing, it is essential to provide some form of chemical barrier layer between the PZT film and the GaAs substrate. A further difficulty is that, in contrast with the thermally grown SiO_2 buffer layer on Si, the native oxides present on GaAs are not of sufficient thermal stability to prevent the Ga–As species from out-diffusing at high temperatures.

The effects associated with Ga–As out-diffusion are twofold: firstly the underlying semiconductor device performance may be affected by dopant profile–abrupt-junction smearing; secondly, out-diffusion of Ga–As species into subsequent electrodes and ceramic layers may impair the crystallization and electrical properties of the PZT film. In III–V semiconductor technology, silicon nitride (Si_3N_4) has been shown to be an effective barrier to outdiffusion of Ga–As species from GaAs when heat treated at temperatures up to 900 °C [8, 9]. Literature concerning the hybridization of GaAs with ferroelectric perovskites such as $PbTiO_3$, $Pb(Zr, Ti)O_3$ or $BaTiO_3$ is limited [10, 11]. It has been reported that conventional furnace firing of a lead titanate ($PbTiO_3$), thin film on a $Pt/Ti/Si_3N_4/GaAs$ substrate at 600 °C resulted in Ga–As diffusion into the $PbTiO_3$ film [11]. Thermal expansion mismatched between the GaAs substrate and PZT thin film have also been proposed as a mechanism for poor-quality thin films of PZT on platinized GaAs substrates [12]. This is because the value of the thermal expansion coefficient, α, of GaAs does not follow that of PZT, as Si does, over the entire firing range, 0–700 °C.

The purpose of the present work was to establish the possibility of depositing crack-free PZT films 0.5 μm thick on a $Si_3N_4/GaAs$ substrate by applying a single coating of a propanediol sol. In addition to using a Si_3N_4 barrier layer to isolate the PZT from the GaAs, rapid thermal processing (RTP) techniques have been adopted in a further attempt to avoid problems of Ga–As out-diffusion that could destroy the piezoelectric properties of the ceramic film.

2. Experimental procedure

All processing including sol deposition was performed in a class 100 clean-room environment. The preparation of the platinized GaAs substrates can be divided into two stages: passivation and metallization. Passivation of the GaAs substrate was achieved by plasma-enhanced chemical vapour deposition (PECVD) of 1000 Å of silicon nitride. The substrate was then subjected to a standard anneal at 600 °C for 1 h to remove hydrogen which is incorporated during deposition of the silicon nitride layer; silicon nitride deposited via PECVD has typically 25% hydrogen and has the empirical formula $SiN_{0.9}H_{0.6}$. This anneal is essential since any out-diffusion of hydrogen during high-temperature processing of subsequent overlayers may lead to damage in these layers. Prior to Ti evaporation the silicon nitride surface was cleaned in a dilute $HF:H_2O$ (1:50) solution for 5 s. Metallization involved thermal evaporation of titanium, oxidation of the titanium, and electron-beam evaporation of platinum. All evaporations were performed under high-vacuum conditions, i.e., less that 10^{-6} Torr. A 50 Å layer of Ti was thermally evaporated onto the Si_3N_4 at approximately 5 Å s^{-1}. The samples were then removed from the evaporator and annealed *ex situ* in air at 650 °C for 10 s in order to oxidize the Ti to TiO_2 [13]. The samples were then placed back into the evaporation system and a Pt layer 1000 Å thick was electron-beam evaporated onto the TiO_2 at approximately 20 Å min^{-1}. The Pt metallization functions as the bottom electrode for the PZT device. The samples were then retrieved from the evaporator for immediate sol–gel deposition.

Films of PZT (53/47) having a thickness of 0.5 μm were produced using the diol-based sol–gel route developed by Phillips *et al.* [14]. Gel-precursor solutions (sols) for PZT (53/47) were prepared from lead acetate trihydrate ($Pb(CH_3COO)_2 \cdot 3H_2O$), titanium diisopropoxide bispentanedionate, ($Ti(OC_3H_7)_2(CH_3COCHCOCH_3)_2$) and zirconium *n*-propoxide ($Zr(n\text{-}OC_3H_7)_4$) stabilized with pentanedione. The solvent was 1,3-propanediol ($HOCH_2CH_2CH_2OH$). The sol was made with 10 mol% excess $Pb(CH_3COO)_2$; *n*-propanol was used as the solvent to dilute the stock solution to 1 M. The details of the sol preparation process have been described elsewhere [15].

The sols were delivered onto a stationary host substrate ($Pt/TiO_2/Si_3N_4/GaAs$) via an in-line 0.2 μm syringe filter to avoid particulate contamination. The substrates were then spun at 2500 rev min^{-1} for 1 min to spin off excess sol and to produce a uniform coating. Prior to annealing, the volatile organic compounds have to be removed from the film. This was initially achieved by heating the films at 350 °C for 1 min in a rapid thermal annealer to give optimal quality using the diol-based route [15]. Crystallization of the PZT into the required perovskite crystal structure was then brought about by further rapid thermal processing of the sample at 650 °C for 10 s at a heating rate of approximately 50 °C s^{-1}. The temperature of the samples was monitored using a chromel–alumel thermocouple in proximity to the sample being processed.

The microstructure and thickness of the films were examined using a Hitachi S700 scanning electron microscope. The films were structurally characterized by X-ray diffraction (XRD) using a Phillips APD 1700 diffractometer. Ferroelectric capacitors were formed in order to perform low-frequency polarization–electric field intensity (*P–E*) measurements by defining Au(1000 Å)/Ti(50 Å) dots of 0.5 mm diameter on the $PZT/Pt/TiO_2/Si_3N_4/GaAs$ structures using standard photolithographic–thermal evaporation methods. The platinum electrode back contact was revealed using photolithography and etching the PZT thin film with a 50 vol% aqueous solution of tetrafluroboric acid (HBF_4).

A Radiant Technologies RT66A ferroelectric analyser system was used to obtain the low-frequency (60 Hz) polarization versus electric field intensity results. Dielectric measurements were obtained using a Hewlett–Packard 4192A impedance analyser at 2 kV cm^{-1} root mean square and 1 kHz. At least three measurements from different surface electrodes were taken.

3. Results and discussion

A cross-sectional scanning electron micrograph of the $PZT/Pt/TiO_2/Si_3N_4/GaAs$ structure indicated a uniform PZT film thickness of 0.5 μm (Fig. 1a). The grain size at the film surface was less than 0.1 μm, as shown in Fig. 1b.

All films prepared by a single deposition of a 1 M sol were found to be free from cracks which can arise owing to the stresses generated during the conversion of the gel coating to a dense ceramic film, and because of thermal expansion mismatches between film and substrate. The ability of the diol sols to resist such stresses is thought to be due to the linear nature of the polymeric precursor molecules making the gels more compliant than other gel types. The surface of the film revealed an uneven surface topography, which we have never seen in corresponding samples on platinized silicon; this may be indicative of hillocks forming in the underlying Pt layer [16]. In some samples, problems of film delamination occurred, although oxidizing the Ti before depositing the Pt layer reduced the frequency with which this occurred. Further work is in progress to improve the reproducibility of our metallization procedures so as to attain a greater batch-to-batch consistency and to reduce the failure rate due to film delamination during firing.

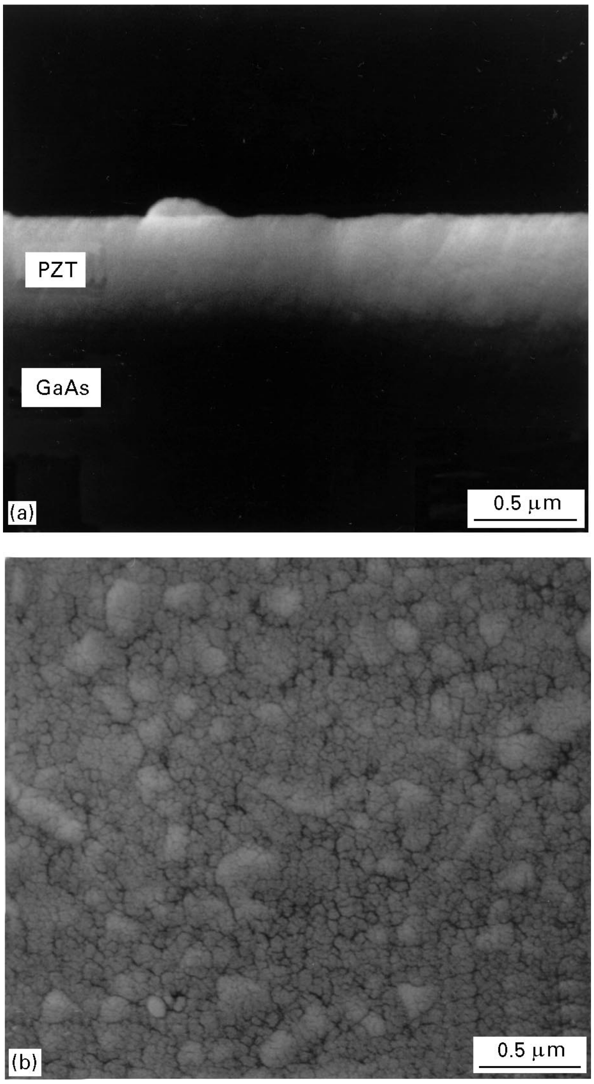

Figure 1 (a) Top and (b) cross-section scanning electron micrographs of the rapid thermally processed PZT film on $Pt/TiO_2/Si_3N_4/GaAs$.

The aim of using RTP techniques in this case was to obtain a dense crystalline PZT film whilst restricting the length of time that the film spent at elevated temperatures, so as to minimize problems associated with As–Ga diffusion. Although RTP techniques have been used extensively in GaAs semiconductor processing, [17] their application to the crystallization of ceramic thin films has received less attention [18, 19]. In order to avoid disruption to the film due to rapid expulsion of organic decomposition products during RTP, a pre-treatment at 350 °C was adopted.

The XRD pattern of the film after RTP (Fig. 2) shows that despite the brief heat treatment (650 °C for 10 s) the film had crystallized to the desired perovskite PZT phase. This composition PZT (53/47) lies on the morphotropic phase boundary between rhombohedral and tetragonal phase fields but, because of line broadening effects, thin-film samples are commonly indexed on the basis of a pseudocubic pattern. The relative intensities of the (1 0 0), (1 1 0) and (1 1 1) pseudocubic peaks are presented in Table I; for reference purposes the values from an analogous powder pattern are shown.

The data illustrate that, relative to the powder pattern, there is a slight enhancement of the thin-film (1 0 0) peak intensity, and a diminution in the intensity of the (1 1 1) peak. In previous experiments using conventional furnace heat treatments for films deposited using the same sols but on (1 1 1) platinized silicon substrates, a strong preferred orientation in the (1 1 1) direction was observed; the data for such a film are also presented in Table I. The bottom electrodes were similar in each substrate system but there were differences in the metallization conditions, or post-metallization annealing conditions (the platinized silicon was obtained commercially). The XRD pattern of the electroded silicon substrate showed only a Pt (1 1 1) peak, whereas for the GaAs substrate there was a strong

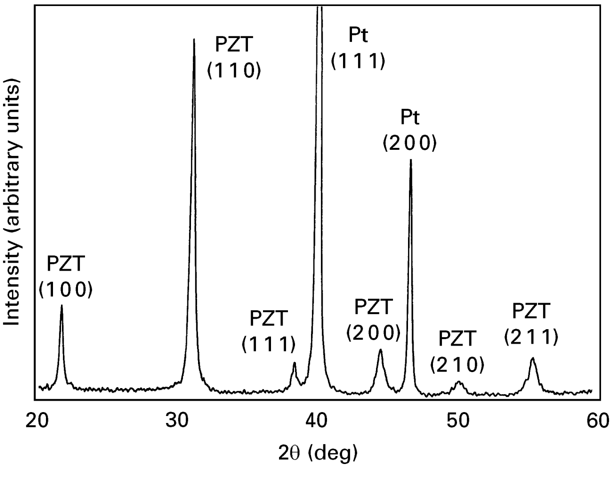

Figure 2 XRD pattern of intensity versus 2θ for the $PZT/Pt/TiO_2/Si_3N_4/GaAs$ structure after a RTP heating schedule of 300 °C for 1 min followed by 650 °C for 10 s at a heating rate of about $50\,°C\,s^{-1}$.

TABLE I Relative intensity of XRD peaks for PZT on platinized GaAS ($Pt/TiO_2/Si_3N_4/GaAs$) and platinized Si ($Pt/Ti/SiO_2/Si$) (a PZT powder pattern is included as reference)

(*h k l*)	Relative intensity of XRD peaks		
	PZT on $Pt/TiO_2/Si_3N_4/GaAs$	PZT on $Pt/Ti/SiO_2/Si$	PZT powder
(1 0 0)	23	20	17
(1 1 0)	100	80	100
(1 1 1)	8	100	14

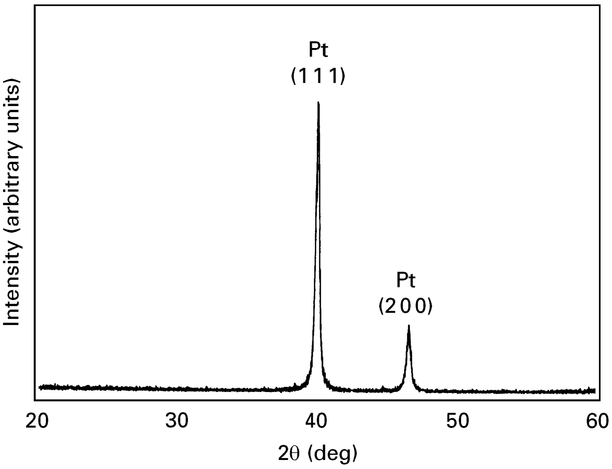

Figure 3 XRD pattern of intensity versus 2θ for the as-deposited $Pt/TiO_2/Si_3N_4/GaAs$ substrate.

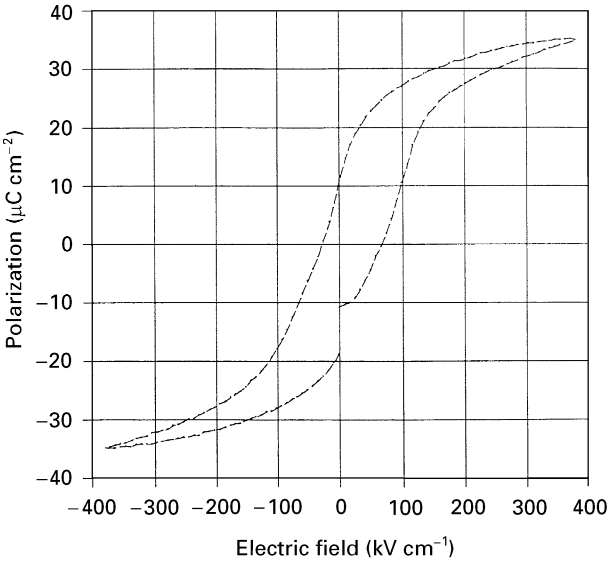

Figure 4 Polarization versus electric field intensity (*P–E*) hysteresis measurements on $Au/Ti/PZT/Pt/TiO_2/Si_3N_4/GaAs$ ferroelectric capacitors.

(1 1 1) reflection together with a weaker (2 0 0) reflection (Fig. 3). Lattice matching between Pt and PZT and the consequent heterogeneous nucleation of PZT promotes (1 1 1) orientation in conventionally heat-treated propanediol sol–gel PZT films on platinized silicon [15]. However, interactions between the Pt and the underlying Ti adhesion layer and between Pb and Pt make for a rather complex electrode system, leading for example to the formation of Pt_3Ti and $PbPt_x$ phases which are of even closer lattice spacing to PZT(53/47) and are likely to play an important role in the nucleation and growth of (1 1 1)-oriented PZT crystallites. In the present work we think it unlikely that the slight difference in electrode structure between platinized $Si_3N_4/GaAs$ and platinized SiO_2/Si used in the previous experiments would account for the observed differences in PZT preferred orientation.

The RTP technique used in the present study involved heating the films from the top surface by means of quartz lamps; the lack of (1 1 1) orientation is therefore consistent with crystallization commencing at the film surface or occurring within the bulk of the film so that the structure of the bottom electrode does not control the orientation of the crystallizing PZT. However, as already mentioned, scanning electron microscopy (SEM) implied that hillocks may have formed in the underlying Pt; this physical disruption to the Pt and the PZT would override any preferred orientation effects and may explain the lack of (1 1 1) orientation in the films. It has been seen recently that annealing of $Pt/Ti/SiO_2/Si$ and $Pt/TiO_2/SiO_2/Si$ substrates does result in hillock formation on the platinum surface [16]. The existence of a slight (1 0 0) orientation in the PZT films in this study may simply be indicative of a self-texture mechanism [20].

Commonly a residual pyrochlore phase is present in sol–gel-deposited PZT, giving rise to a broad extra XRD peak at $2\theta = 29.5°$. The pyrochlore phase is an intermediate crystallization product in conventionally fired samples. In our rapidly fired samples there was no evidence of this peak (Fig. 2), indicating either that the gel layer transformed directly to perovskite PZT or that, if an intermediate structure was formed, it was sufficiently unstable so as to transform to the desired perovskite phase within the short heating cycle employed, 650 °C for 10 s. Reports in the literature using RTP for PZT films on $Pt/Ti/SiO_2/Si$ suggest that the latter explanation is correct since other workers have shown that, for dwell times of 1–5 s at 600 °C, a pyrochlore phase (thought to be $Pb_2(Zr_{0.53}Ti_{0.47})_2O_6$) was detected together with the perovskite phase whereas, for longer heating times, only the perovskite phase was detected [21]. A faint extra peak at a $2\theta = 22.5°$ is probably due to an interfacial reaction at the bottom electrode, but this peak has not been identified unambiguously.

The polarization–electric field response, shown in Fig. 4, is consistent with ferroelectric switching behaviour, with spontaneous polarization values of 37 μC cm^{-2}. The average remanent zero-field polarization, $(|_+P_r| + |_-P_r|)/2$, was 14 μC cm^{-2}, with a corresponding average coercive field, $(|_{+}E_c| + |_{-}E_c|)/2$, of 47 kV cm^{-1}. Average values are quoted as the loops were displaced along the positive field axis, giving rise to non-equivalent parameters in the positive and negative cycles. Such an effect is indicative of an internal bias field; in the positive cycle, this field acts in sympathy with the externally applied field and against it in the reverse cycle pulse. Actual measured values of coercive fields were $+E_c = 70$ kV cm^{-1} and $-E_c = 25$ kV cm^{-1} with a loop displacement of 22 kV cm^{-1}. Corresponding remanent polarization values were $+P_r = 11$ μC cm^{-2} and $-P_r = 18$ μC cm^{-2}, but this asymmetry in remanent polarization is a consequence of the displacement of the loop along the field axis (positive and negative spontaneous polarization values were equivalent).

An internal bias field in ferroelectric materials is commonly associated with the reorientation with respect to the direction of spontaneous polarization of dipoles formed by acceptor ion impurity–oxygen vacancy pairs [22]. In the case of PZT, orientation of oxygen vacancy–lead vacancy pairs may also make an important contribution. Other possible mechanisms for the development of internal bias fields and displaced hysteresis loops include the migration of defects to domain boundaries and electrodes. In the present work it is possible that Ga and As diffusion and interfacial reactions at the bottom electrode are likely to bring about changes in the electrical behaviour of the bottom electrode producing an asymmetric electrode system which contributed to an asymmetric *P–E* response.

The measured polarization values were significantly lower than the 20–30 μC cm^{-2} values that are typical for corresponding films fired coventionally on platinized silicon. This could be due to incomplete crystallization in the RPT films but further work is required to confirm the precise reason(s). Possibly longer RTP dwell times would improve the crystallinity of the product but residual problems of As and Ga diffusion cannot be ruled out at this stage.

The low-frequency relative permittivity, ε_r, and dielectric loss tangent, tan δ, of the films were found to be 650 and 0.04, respectively. The value of ε_r is approximately 30% lower than those values observed for PZT thin films on platinized silicon derived by RTP methods [18, 19]; again this may be an effect of interface reactions or possible Ga–As diffusion into the ceramic film.

4. Conclusions

We have produced crack-free PZT thin films on a platinized GaAs substrate system having a Pt/TiO_2/Si_3N_4/GaAs layer structure. The substrate was fabricated using PECVD-processed Si_3N_4 as the Ga–As diffusion barrier in conjunction with a thermally oxidized Ti layer as an adhesion layer. Annealing of the PZT has been performed using RTP techniques. SEM indicated that the grain size of the PZT top surface was less than 0.1 μm. XRD patterns have revealed the required perovskite crystal structure with some evidence of a slight (1 0 0) preferred orientation; no pyrochlore phase was detected. Low-frequency polarization versus electric field intensity hysteresis loops were displaced along the field axis; average values of remanent and spontaneous polarizations were 14 μC cm^{-2} and 37 μC cm^{-2}, respectively, with an average value of coercive field equal to 47 kV cm^{-1} being observed.

Acknowledgements

The authors would like to thank Dr G. Hill, Engineering and Physical Science Research Council (EPSRC) Central Facility for III–V Semiconductor Research, University of Sheffield, for the deposition of the Si_3N_4 films and Mr N. Smith for technical assistance during the electrical measurements. We would also like to acknowledge EPSRC for financial support of the work.

References

1. K.-H. HELLWEGE and A. M. HELLWEGE (eds.), "Ferroelectrics: Oxides", Landolt–Börnstein New Series, Vol. 16, Springer, Berlin, (1981) p. 119.
2. T. W. GRUDKOWSKI, J. F. BLACK, T. M. REEDER, D. E. CULLEN and R. A. WAGNER, *Appl. Phys. Lett.* **37** (1981) 993.
3. S. ARSCOTT, Z. AWANG, Y. L. TU, S. J. MILNE and R. E. MILES, *Ferroelectrics* **187** (1996) **49** (1996).
4. G. R. KLINE and K. M. LAKIN, *Appl. Phys. Lett.* **43** (1993) 750.
5. C. J. BRINKER and G. W. SCHERER, 'Sol–gel science: the physics and chemistry of sol–gel processing" (Academic Press, Boston, MA, 1990).
6. M. J. BOZACK, J. R. WILLIAMS, J. M. FERRARO, Z. C. FENG and R. E. JONES Jr, *J. Electrochem. Soc.* **142** (1985) 485.
7. S. B. KRUPANIDHI, N. MAFFIE, M. SAYER and K. EL-ASSAL, *J. Appl. Phys.* **54** (1983) 6601.
8. J. GYULAI, J. W. MAYER, I. V. MICHELL and V. RODRIGUEZ, *Appl. Phys. Lett.* **17** (1970) 332.
9. J. S. HARRIS, F. H. EISEN, B. WELCH, J. D. HASKELL, R. D. PASHLEY and J. W. MAYER, *ibid.* **21** (1972) 601.
10. S. K. DEY and R. ZULEEG, *Ferroelectrics* **112** (1989) 309.
11. R. W. SCHWARTZ, Z. XU, D. A. PAYNE, T. A. DETEMPLE and M. A. BRADLEY, *Mater. Res. Symp. Proc.* **200** (1990) 167.
12. V. SRIKANT, E. J. TARSA, D. R. CLARKE and J. S. SPECK, *J. Appl. Phys.* **77** (1995) 1517.
13. M. J. DONACHIE, Jr. (ed.) "Titanium and titanium alloys" (American Society for Metals, Metals Park, OH, 1982) p. 338.
14. N. J. PHILLIPS, M. L. CALZADA and S. J. MILNE, British Patent Application 9114476.6 (1991).
15. Y. L. Tu and S. J. MILNE, *J. Mater. Sci.* **30** (1995) 2507.
16. H. N. AL-SHAREEF, D. DIMOS, B. A. TUTTLE and M. V. RAYMOND, *J. Mater. Res.* **12** (1997) 347.
17. R. SINGH, *J. Appl. Phys.* **63** (1988) R59.
18. C. V. R. VASANT KUMAR, R. PASCUAL and M. SAYER, *ibid.* **71** (1992) 846.
19. J. CHEN, K. R. UDAYAKUMAR, K. G. BROOKS and L. E. CROSS, *ibid.* **71** (1992) 4465.
20. T. TANI, Z. XU and D. PAYNE, *Mater. Res. Soc. Symp.* **310** (1993) 269.
21. K. G. BROOKS, I. M. REANEY, R. KLISSURSKA, Y. HUANG, L. BURSILL and N. SETTER, *J. Mater. Res.* **9** (1994) 2540.
22. P. V. LAMBECK and G. H. JONKER, *J. Phys. Chem. Solids*, **47** (1986) 453.

Received 22 April
and accepted 17 June 1997